ELSEVIER

Polymer 43 (2002) 3061–3068

polymer

www.elsevier.com/locate/polymer

Two-stage sorption in rubbery semicrystalline polymers: transport of primary alcohols in polyesteramide

M.S. Hedenqvist*, M. Krook[1], U.W. Gedde

Department of Polymer Technology, Royal Institute of Technology, SE-100 44 Stockholm, Sweden

Received 19 November 2001; accepted 8 February 2002

Abstract

This paper deals with the two-stage sorption of methanol, 1-propanol and 1-hexanol in a rubbery semicrystalline polyesteramide. This is the first time two-stage sorption is reported for a semicrystalline rubbery polymer. Mass uptake, specimen geometry and surface concentration were measured independently. The two-stage sorption curve describes two overlapping processes; a very rapid diffusion (mode 1) superimposed onto a normal s-shaped sorption curve (mode 2). Mode 1 swelling was uni-dimensional and mode 2 swelling was initially uni-dimensional and later three-dimensional. It was possible to model the sorption curves by assuming time-dependent solute-surface-concentration conditions, similar to those used to describe simple s-shaped sorption. The obtained time dependence, characterised by a single relaxation time, agreed with experimental values of the surface concentration obtained by infrared spectroscopy. The relaxation time increased exponentially with increasing size of the diffusing alcohol molecule. The solubility of the alcohols in the polymer increased with increasing hydroxyl-group density. The diffusivity of alcohol decreased nonlinearly with increasing length of the molecule, size effects being less important for larger solutes.

Keywords: Two-stage sorption; Alcohols; Polyesteramide

1. Introduction

S-shaped sorption curves are commonly observed when polymers are exposed to a swelling solute [1]. These can be adequately described by time-dependent surface solute concentrations [1]. Occasionally, two-stage rather than s-shaped sorption behaviour is observed [2]. This behaviour has been reported almost exclusively for solute–polymer systems where the dry polymer is glassy [3–8]. However, two-stage sorption may also occur in rubbery polymers [9]. Two-stage sorption in glassy polymers has been explained by the presence of two competing processes: Fickian diffusion and polymer relaxation. At short times, local rapid polymer molecular rearrangements dominate and the system is diffusion-controlled (first stage). Slow large-scale molecular rearrangements prevail in the second stage and in this stage the system is relaxation-controlled [8]. The two-stage process has also been explained by the occurrence of solute (water) clustering and polymer free volume redistribution during sorption, both of which mean that the diffusivity decreases with time [3]. Several models have been used to reproduce the two-stage curve. In the 'variable surface-concentration model' (VSC), it is assumed that the solute concentration at the surface reaches a given value instantaneously (first stage) and that the final surface concentration is reached at a rate given by a first-order relaxation process (second stage) [4,10].

In the 'diffusion-relaxation model' of Berens and Hopfenberg [11], it is assumed that the rate of sorption is the result of a linear superposition of two processes: one described by ordinary 'Fickian diffusion' and another described by polymer mechanical relaxation. The second process is described by the summation: $\sum_i M_{\infty,i}(1 - e^{-(t/\tau_i)})$, in order to account for the broad spectrum of relaxation times for polymers. $M_{\infty,i}$ is the final mass uptake due to the ith relaxation process with relaxation time τ_i. The 'diffusion-reaction model' is similar to VSC in that the surface solute concentration has the same time dependence [12]. The diffusion-reaction model is also similar to the dual-mode sorption concept, in that it considers that the solute population consists of mobile and immobile species. The distribution of the two species is governed by first-order reversible reaction kinetics. The instantaneous surface concentration corresponds to the equilibrium concentration of the mobile species and the final equilibrium concentration is

* Corresponding author. Tel.: +46-8-790-7645; fax: +46-8-20-8856.
E-mail address: mikaelhe@polymer.kth.se (M.S. Hedenqvist).
[1] The Foundation Packforsk—The Swedish Packaging Research Institute, P. O. Box 9, SE-164 93 Kista, Sweden.

0032-3861/02/$ - see front matter
PII: S0032-3861(02)00137-4

Nomenclature

C	solute concentration
C_∞	saturation solute concentration
C_{i1}	solute concentration associated with mode 1
C_{i2}	initial solute concentration associated with mode 2a
$D(C)$	concentration-dependent diffusivity
D_{coi}	zero concentration diffusivity of mode i
d_p	depth of IR penetration
err	integration error in the Runga–Kutta method
F_0	rate of evaporation
h	step length in the spatial direction
I	indentity matrix
i	integer number of the spatial position
j	integer number of the time position
k_1,k_2,k_3	constants in the Runge–Kutta method
L	thickness of half the plate
$m+1$,m,mp	indices for next, actual and previous iteration steps
n	number of x-coordinates
n_i	refractive index of the ATR crystal (1) and the polymer (2)
T	temperature
t	time
T_1	time of the first plateau
tol	absolute tolerance for the Runga–Kutta integration
tol1	relative tolerance for the Runga–Kutta integration
V_1	solute molar volume
w_1	saturation solute mass fraction
x	space coordinate
α_i	constant describing the magnitude of concentration dependence of Din mode i
λ	wavelength
θ	angle of incidence
τ	surface concentration relaxation time

determined by the relative population, at equilibrium, of mobile and immobile solute molecules.

In the only study, to our knowledge, of two-stage behaviour in rubbery polymers [9], it was suggested that two-stage behaviour is observed when solute diffusion and polymer-relaxation rates are of similar orders of magnitude. The study involved, however, a large molecule (phenyl ethyl alcohol) in a relatively 'rigid' and dense rubber (bromobutyl rubber). Thus, reports on two-stage behaviour in rubbery polymers are scarce and the phenomenon has not been revealed for rubbery semicrystalline polymers. This work aims to explain the two-stage behaviour in rubbery semicrystalline polymers and specifically in the case of a hydrogen-bonding polymer (polyesteramide) exposed to hydrogen-bonding solutes (methanol, 1-propanol and 1-hexanol). In order to reveal the mechanisms behind the two-stage sorption in these systems, the sorption/desorption curves are modelled by finite difference algorithms using Fick's law with solute-concentration-dependent diffusivity and time-dependent solute surface concentration, the latter being measured in situ by infrared spectroscopy. Additionally, the mass uptake during sorption is coupled with independent measurements of the specimen geometry.

2. Experimental

2.1. Materials

Bayer kindly supplied an experimental grade of the polyesteramide, BAK 404-004 (referred to as BAK), Fig. 1. The polymer had a density of 1160 kg m^{-3} at 20 °C, $\bar{M}_w$ = 37 400 g mol^{-1} and a melting point in the range from 115 to 125 °C. The polymer is considered to be biodegradable according to DIN 54900. Methanol (purity: >99.8%), 1-propanol (purity: >99.5%) and 1-hexanol (purity: >98%) were obtained from E. Merck AB, Sweden. These alcohols are hereafter referred to simply as methanol, propanol and hexanol, respectively.

2.2. Sorption and desorption measurements

The sorption experiment was carried out by immersing sheets (40 mm × 40 mm with a thickness of 0.45–0.5 mm) in the liquid alcohol at 25 °C. The weight increase was recorded by intermittently weighing the sheets using a Mettler-Toledo AE 163 balance. The solute-saturated sheets were exposed to air at 25 °C and the desorption kinetics were monitored by intermittent weighing of the samples on a Mettler-Toledo AE 163 balance.

2.3. Infra-red-spectroscopy

A Perkin–Elmer 2000 FTIR-spectrophotometer, equipped with a Golden Gate accessory from Grasseby Specac, was used to obtain reflection-Infra-red (IR)-spectra.

3. Theory

Fick's second law of diffusion, which can be expressed as

$$\frac{\partial C}{\partial t} = \frac{\partial}{\partial x}\left(D(C)\frac{\partial C}{\partial x}\right) \quad (1)$$

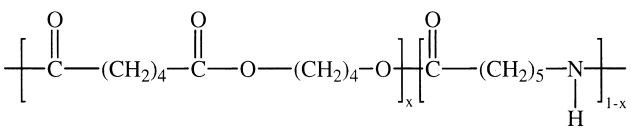

Fig. 1. The chemical structure of BAK [21].

was solved for a plate geometry where C is the penetrant concentration (g cm^{-3}), x the thickness coordinate and t is the time. Only half the plate thickness was considered, and the inner boundary coordinate was described as an isolated point:

$$\left(\frac{\partial C}{\partial x}\right)_{x=L} = 0 \tag{2}$$

The outer boundary was allowed to take any type of function. During desorption, evaporation takes place at the surface:

$$D(C)\left[\frac{\partial C}{\partial x}\right]_{x=0} = F_0 C \tag{3}$$

where F_0 is the evaporation constant determined to be 7.18×10^{-5} cm s^{-1} for methanol using a procedure described by Bakhouya et al.[13]. In contrast to methanol, the propanol and hexanol systems were diffusion-controlled rather than evaporation-controlled and thus F_0 was set equal to infinity in their cases. The concentration-dependent diffusivity was described as:

$$D(C) = D_{\mathrm{co}}\, \mathrm{e}^{\alpha C} \tag{4}$$

where D_{co} is the zero concentration diffusivity and α is the plasticisation power. Implementing Eq. (4), Eq. (1) is discretized according to:

$$\frac{\partial C}{\partial t} = f(t, C) = \frac{D_{\mathrm{co}}}{\Delta x_i^2}(\mathrm{e}^{\alpha C_{i+0.5}}(C_{i+1} - C_i) - \mathrm{e}^{\alpha C_{i-0.5}}(C_i - C_{i-1})) \tag{5}$$

where

$$C_{i\pm 0.5} = \frac{C_i + C_{i\pm 1}}{2} \tag{6}$$

Eq. (2) is best discretized using

$$C_{n+1} = C_{n-1} \tag{7}$$

($i = n$ at the centre of the plate), and the surface boundary condition (Eq. (3)) may be written explicitly, including Eq. (4)), as ($i = 0$ at the boundary):

$$C_0 = \frac{C_1}{1 + \dfrac{\Delta x_i F_0}{D_{\mathrm{co}}\, \mathrm{e}^{\alpha C_1}}} \tag{8}$$

The concentration profiles were generated using the following implicit multi-step method [14–16]:

$$\nabla^3 C_{j+1} = \frac{6}{11} h_j \left(f(t_{j+1}, C_{j+1}) - \frac{1}{h_j}\left(\frac{3}{2}\nabla^2 C_j + \nabla C_j\right)\right) \tag{9}$$

which was derived from the multi-step formula [15]:

$$\frac{1}{3}\nabla^3 C_{j+1} + \frac{1}{2}\nabla^2 C_{j+1} + \nabla C_{j+1} = h_j f(t_{j+1}, C_{j+1}) \tag{10}$$

where C_{j+1} is calculated from:

$$C_{j+1} = \nabla^3 C_{j+1} + \nabla^2 C_j + \nabla C_j + C_j \tag{11}$$

using the Nordsieck matrix of differences [15] ($\nabla^3 C_{j+1} = \nabla^2 C_{j+1} - \nabla^2 C_j$, etc.). The implicit method integrates with respect to time using arcs with three constant time steps but with a variable step size between them. After the last step of each arc, the local error is estimated and a new step size is selected. The predictor–corrector procedure for solving the implicit Eq. (9) is of the Newton-type:

$$\nabla^3 C_{j+1}^{(m+1)} = \frac{\nabla^3 C_{j+1}^{(mp)}}{F'(C)} \tag{12}$$

where $\nabla^3 C_{j+1}^{(mp)}$ is calculated from Eq. (9) using:

$$C_{j+1} = \nabla^2 C_j + \nabla C_j + C_j \tag{13}$$

$$F'(C) = I - \frac{6h_i}{11}\left(\frac{\partial f(t, C)}{\partial C}\right) \tag{14}$$

where I is the identity matrix. $(\partial f(t, C)/\partial C)$ is the Jacobian matrix (Eqs. (15)–(17)) and is calculated at the first arc point in the arc from the difference scheme given in Eq. (5):

$$\frac{\partial f(t, C)}{\partial C_{i-1}} = \frac{D_{\mathrm{co}}}{\Delta x^2}\left(\frac{\alpha}{2}\mathrm{e}^{\alpha C_{i-0.5}}(C_i - C_{i-1}) - \mathrm{e}^{\alpha C_{i-0.5}}\right) \tag{15}$$

$$\frac{\partial f(t, C)}{\partial C_i} = \frac{D_{\mathrm{co}}}{\Delta x^2}\left(\frac{\alpha}{2}\mathrm{e}^{\alpha C_{i+0.5}}(C_{i+1,} - C_i) - \mathrm{e}^{\alpha C_{i+0.5}} - \frac{\alpha}{2}\mathrm{e}^{\alpha C_{i-0.5}}(C_{i,} - C_{i-1}) - \mathrm{e}^{\alpha C_{i-0.5}}\right) \tag{16}$$

$$\frac{\partial f(t, C)}{\partial C_{i+1}} = \frac{D_{\mathrm{co}}}{\Delta x^2}\left(\frac{\alpha}{2}\mathrm{e}^{\alpha C_{i+0.5}}(C_{i+1,} - C_i) + \mathrm{e}^{\alpha C_{i+0.5}}\right) \tag{17}$$

The last point in the arc is corrected twice using Eq. (12) followed by Eq. (18)

$$\nabla^3 C_{j+1}^{(m+1)} = \nabla^3 C_{j+1}^{(mp)} + \frac{\nabla^3 C_{j+1}^{(m)} - \nabla^3 C_{j+1}^{(mp)}}{F'(C)} \tag{18}$$

where $\nabla^3 C_{j+1}^{(m)}$ is calculated using Eqs. (9) and (11). The first arc is produced by a three-stage second-order Runge–Kutta method [16]:

$$k_1 = f(t_j, C_j) \tag{19}$$

$$k_2 = f(t_j + \Delta t_j, C_j + \Delta t_j k_1) \tag{20}$$

$$k_3 = f(t_j + 0.5\Delta t_j, C_j + 0.25\Delta t_j[k_1 + k_2]) \tag{21}$$

If the error:

$$\mathrm{err} = \Delta t_j \frac{k_1 - 2k_3 + k_2}{3} \tag{22}$$

is less than the tolerance:

$$\mathrm{tol} = \mathrm{tol1} \times \max(C_j, 1) \tag{23}$$

where tol1 is the relative tolerance kept at 0.001, the

solution is updated:

$$t_{j+1} = t_j + \Delta t_j \tag{24}$$

$$C_{j+1} = C_j + \Delta t_j \frac{k_1 + 4k_3 + k_2}{6} \tag{25}$$

Otherwise, a smaller step size is selected and the scheme (Eqs. (19)–(23)) is computed again. The new step size is determined according to:

$$\Delta t_{j+1} = \min\left(\Delta t_{\max}, 0.9\Delta t_j \left[\frac{\text{tol}}{\text{err}}\right]^{1/3}\right) \tag{26}$$

where $\Delta t_{\max}$ is the maximum step size allowed. The concentration profiles were integrated using Simpson's method with the Romberg routine to obtain greater accuracy.

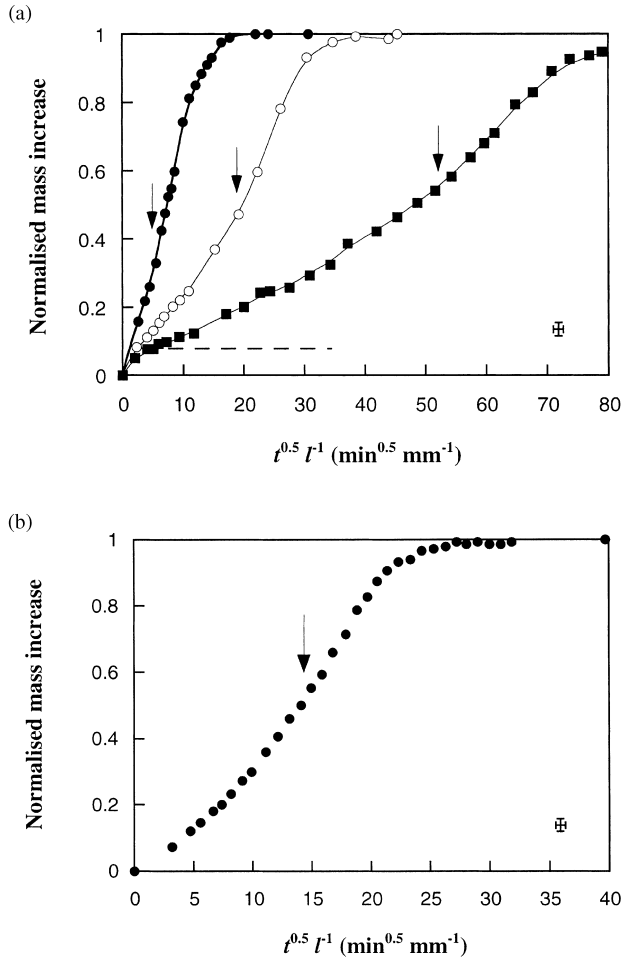

Fig. 2. (a) Normalised mass increase as a function of time for BAK immersed in methanol (●), propanol (○) and hexanol (■). Broken line indicates the approximate position of the plateau. Arrows indicate the approximate place of the transition from mode 2a to mode 2b. (b) Normalised mass increase as a function of time of medium-density polyethylene immersed in *n*-hexane (●). Arrow indicate the approximate position of the transition from stage I to stage II (mode 2a to mode 2b).

4. Results and discussion

The sorption curves of methanol, propanol and hexanol in the BAK polymer showed a two-stage character (Fig. 2a). A rapid initial mass increase was followed by a plateau, followed by a slower mass increase as a function of the square root of time. It appeared that an initial rapid uptake was superimposed onto a simple s-shaped sorption curve, the latter being the type of curve normally observed for rubbery polymers exposed to swelling solutes in the absence of strong interactions (Fig. 2b). The rapid initial uptake, here referred to as mode 1, was associated with only a uni-directional swelling in the thickness direction of the plate without lateral expansion of the specimen (Fig. 3). The same pattern of geometrical changes of the specimens was observed on immersion of all alcohols, but because of the relatively low degree of mass uptake and swelling for propanol and hexanol, these values were coupled with large scatter. Consequently, only the methanol-induced swelling was analysed in detail. The expansion in the plane of the plate was noticeable first after the plateau had been reached, and it accelerated, on a square-root-of-time scale, when entering mode 2b at the first inflection point of the sorption curve. The 'acceleration' was accompanied by a 'thickness-stabilisation' or even by a decrease in thickness.

In order to model the two-stage behaviour, the mass uptake of mode 1 was first subtracted from the sorption curve to yield a 'reduced sorption curve'. The reduced sorption curve showed the typical s-shape and was readily described by a time-dependent surface concentration similar to the VSC-model discussed in the introduction (Fig. 4a–c):

$$C(t) = C_{i2} + (C_\infty - C_{i2})(1 - e^{-(t/\tau)}) \tag{27}$$

where C_{i2} is the initial mass uptake associated with

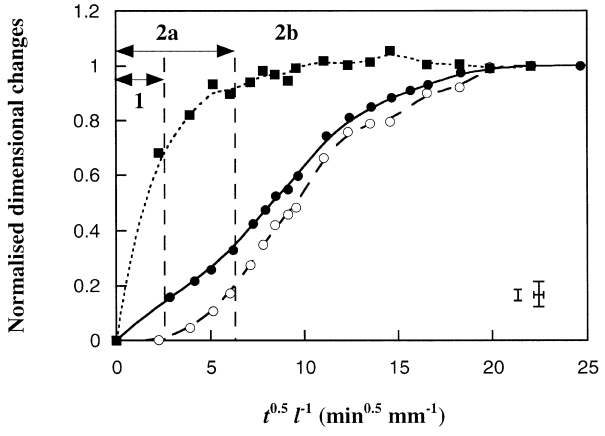

Fig. 3. Normalised mass increase (●), normalised thickness increase (■) and normalised cross-sectional area increase (○) of a BAK plate immersed in methanol. The three modes 1, 2a and 2b are also indicated. The smaller *y*-error bars refer to the normalised mass increase values. The transition between stages 2a and 2b occurred at the first inflection point of the mass increase curve.

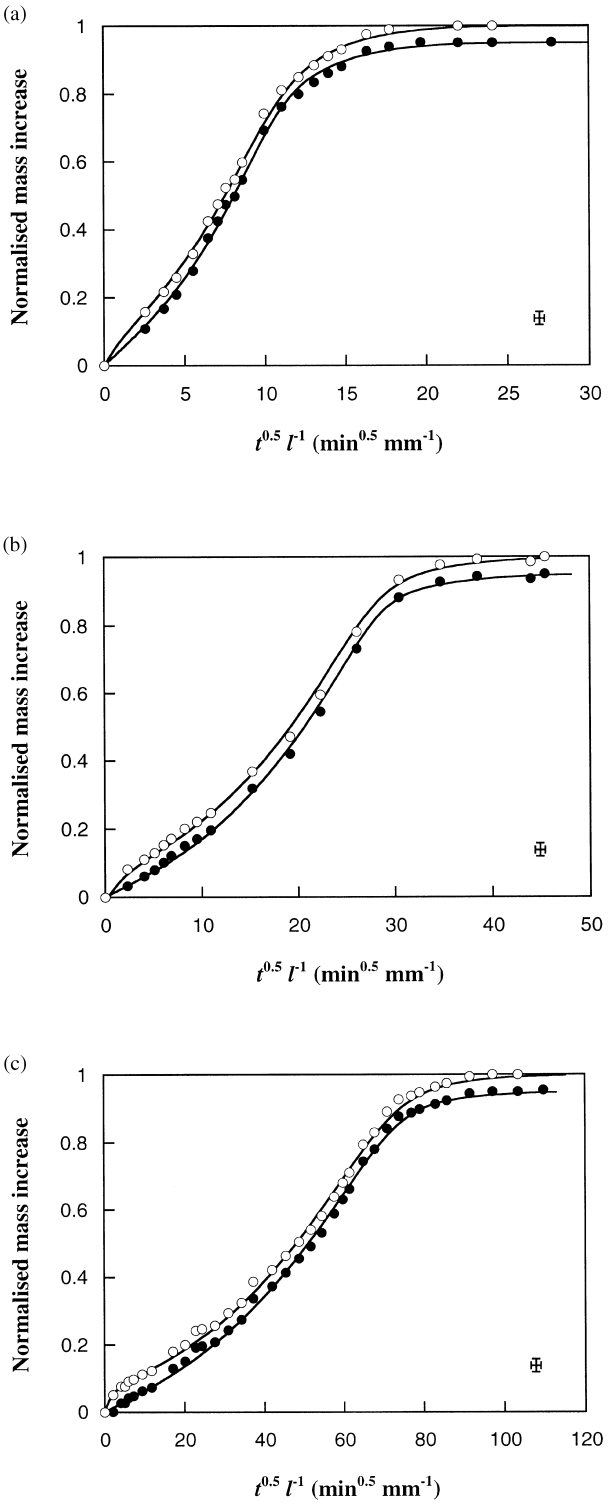

Fig. 4. (a) Normalised mass increase as a function of time of BAK in methanol. (●) indicates experimental data where the mass uptake referring to mode 1 was withdrawn from the sorption curve, and the line corresponds to the numerical fitting presented in the theory part, including Eq. (27). (○) indicates the original experimental data, and the line corresponds to the numerical fitting using the same equations but with mode 1 included. (b) Normalised mass increase as a function of time for BAK in propanol. Symbols and lines as in (a). (c) Normalised mass increase as a function of time for BAK in hexanol in BAK. Symbols and lines as in (a).

mode 2a and C_∞ is the equilibrium concentration. τ is the time constant, 'surface concentration relaxation time' that determines the rate at which the concentration goes from C_{i2} to C_∞. The desorption curves were first fitted to yield D_{co} and α, which were used as input parameters in the fitting of the sorption curves (Table 1). The fitting of the reduced sorption curves yielded C_{i2} and τ, as well as adjusted D_{co} and α values (Table 1). Most of the adjusted sorption D_{co} and α values were lower than the corresponding values obtained from desorption data, an indication that a slow 'loosening up of the structure' due to molecular rearrangements occurred during the sorption/desorption cycle. Fig. 5 shows the zero-concentration diffusivities (D_{co2}) of the alcohols in BAK together with those of primary alcohols in polyamide 6 and *n*-paraffins in polyethylene. The latter two systems were included because they represent, respectively, semicrystalline hydrogen-bonding and non-polar systems. The effect of solute size on the diffusivity decreases with increasing solute size for all systems, but the methanol-BAK value deviated slightly from the general trend. The reason for that is not obvious.

Table 1 shows that the plasticisation power (α_2) increased with the size of the solute, in accordance with the free volume theory [17]. Both τ and C_{i2} increased with increasing size of the alcohol molecule but the change in C_{i2} was very small (Fig. 6, Table 1). The equilibrium concentration (volume fraction) of the alcohols increased with increasing concentration of hydroxyl groups, referring to the pure liquids (Fig. 7). This is due to both the increasing polarity >(enthalpic reasons) and the smaller solute size (steric effects) with increasing hydroxyl concentration. Interestingly, the values follow the solid line that predicts a negligible solute concentration in the polymer if hydroxyl groups are absent, or alternatively if the solute molecule is infinitely large.

The parameters obtained from the fitting of the reduced sorption curves were used as input parameters when fitting the original two-stage sorption curves. It was found that these values could by used unaltered to describe modes 2a and 2b of the two-stage curves (Fig. 4a–c). The only modification necessary in the modelling was to account for the rapid initial mass uptake (mode 1). Here both a constant diffusivity and a highly concentration-dependent diffusivity were used and it was impossible to see, from the goodness of fit, which of the two was the most appropriate. It was clear, however, that these values were erroneously high (D_{co1}s in Table 1). These very large values, based on the assumption that mode 1 ended at the plateau, indicated that mode 1 must end beyond the plateau. The exact time for the end of mode 1 was, however, impossible to determine.

The modelled solute concentration profiles of the two-stage sorption curve of propanol in BAK are shown in Fig. 8. In a previous study [1], the simple s-shaped sorption

Table 1
Transport properties data

Sample	D_{co1} [a]	α_1 [b]	D_{co2} [c]	α_2 [d]	τ [e]	C_{i1} [f]	C_{i2} [g]	T_1 [h]	w_1 [i]
Desorption[j]									
Met	–		1.7×10^{-7}	8.7					0.56
Pro	–		3×10^{-9}	30					0.20
Hex	–		9.8×10^{-10}	44					0.10
Sorption[k]									
Met	0.08*/0.01	200	7×10^{-8}	5	2.1	0.05	0.58	50	
Pro	0.12*/0.0008	450	3×10^{-9}	22	7.1	0.07	0.62	130	
Hex	0.10*/0.00045	500	6.5×10^{-10}	36	48.7	0.14	0.64	180	

[a] Zero concentration diffusivity ($cm^2\ s^{-1}$) in mode 1. * refers to the fitted values when a constant diffusivity was used. The other values correspond to zero-concentration diffusivities when the diffusivity was considered to be highly concentration dependent.
[b] Plasticisation power in mode 1. Unit: $1/w_1$.
[c] Zero concentration diffusivity ($cm^2\ s^{-1}$) from desorption, or from sorption measurements in the case of modes 2a and 2b.
[d] Plasticisation power from desorption, or from sorption in the case of modes 2a and 2b. Unit: $1/w_1$.
[e] Solute surface concentration relaxation time (h) in Eq. (27).
[f] Surface concentration referring to mode 1, normalised with respect to the saturation concentration.
[g] Initial surface concentration referring to mode 2a (including solutes of mode 1), normalised with respect to the saturation concentration.
[h] Time of first plateau of the sorption curve (s).
[i] Saturation solute mass fraction.
[j] Values from the desorption measurements (met = methanol, pro = propanol and hex = hexanol).
[k] Values from the sorption measurements (met = methanol, pro = propanol and hex = hexanol).

curve was divided into a stage I (uni-dimensional swelling) and a stage II (three-dimensional swelling). The transition between stages I and II occurred at the inflexion point of the sorption curve and corresponded to the instant when the core was plasticised to such an extent that the plate was free to swell equally easily in all the three dimensions. This transition also occurred in the present two-stage curves (mode 2a to 2b) but it was superimposed onto the rapid mass uptake of mode 1. Thus modes 2a and 2b of the two-stage curve correspond to stages I and II of the simple s-shaped sorption curve.

Infrared spectroscopy (IR) was used to assess the solute concentration in the surface region of the plate as a function of sorption time. The penetration depth of IR is wavelength dependent, according to [18]:

$$d_p = \frac{\lambda}{2\pi n_1\left(\sin^2(\theta) - \left(\frac{n_1}{n_2}\right)^2\right)^{0.5}} \quad (28)$$

where λ is the wavelength and n_1 is the refractive index of the ATR-crystal (= 2.4). The refractive index of BAK was estimated from group-addition theories presented by Krevelen [19] to be $n_2 = 1.48$. The angle of incidence (θ) was 40°. The prominent 1050 cm^{-1} C–O stretch of the primary alcohol was used for the determination of concentration [20]. This peak was normalised with respect to the methylene

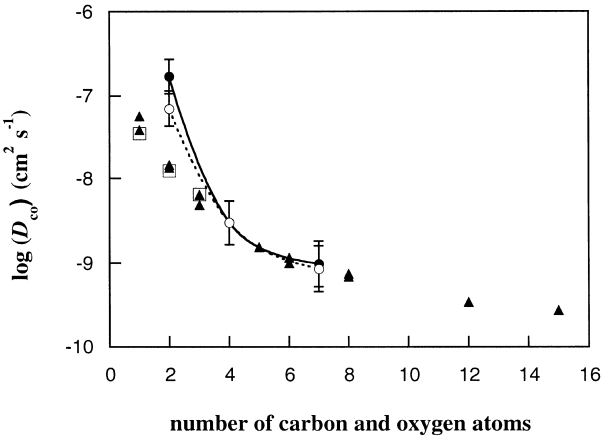

Fig. 5. Zero-concentration diffusivity of the alcohols in BAK from desorption (●) and sorption (○) data as a function of the size of the solute. As a comparison, zero-concentration diffusivities at 25 °C of primary alcohols in polyamide 6 (□) [22] and of *n*-paraffins in polyethylene (▲) [17,23] are shown. The diffusivity values were shifted vertically to match the trend of the propanol and hexanol values of BAK.

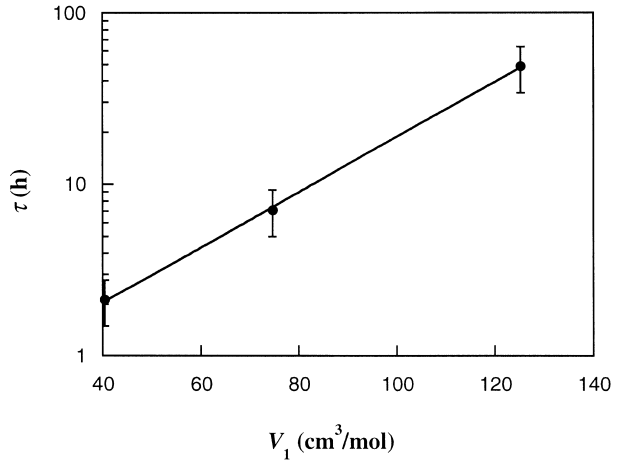

Fig. 6. Surface concentration relaxation time (τ) as a function of the molar volume of the alcohols in BAK.

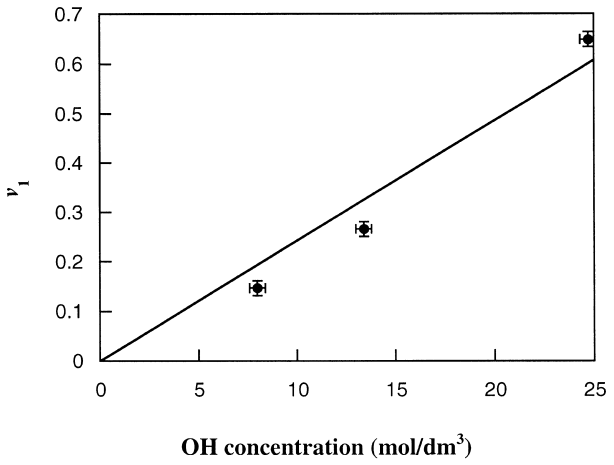

Fig. 7. Equilibrium volume fraction of the alcohols in BAK as a function of the hydroxyl concentration. The solid line represents the best fit of a straight line that has to pass through the orig0.

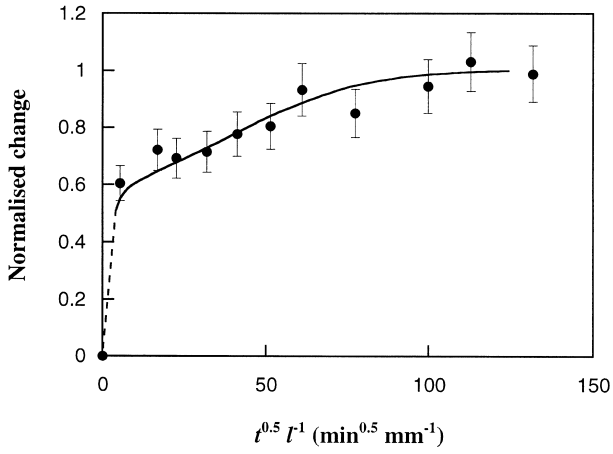

Fig. 9. Normalised absorbance ratio of the 1050 and 2931 cm^{-1} peaks for hexanol in BAK (●). The solid line corresponds to the modelled normalised average concentration of hexanol in the surface (5% of the plate thickness) using the data in Table 1.

C–H stretch at 2931 cm^{-1}. The penetration depths of the two peaks were, according to Eq. (28), 3.6 and 1.3 μm, respectively. These depths corresponded to 7.6 and 2.7% of the plate thickness with an average depth of 5% of the plate thickness. In order to compare the IR-data with the modelling, only the values of the outermost 5% of the simulated concentration profiles were collected. Fig. 9 shows the results obtained by IR-spectroscopy and the modelled surface concentration as a function of time for hexanol. The agreement between the experimental (IR) and modelled surface concentration was very good. The time evolution of the surface concentrations before the plateau of the total sorption curve could not be detected by IR, but the slow approach of the final surface concentration, characterised by τ, was well described by IR. Although the modelling of the time-dependence of the surface concentration in swelling systems has been extensively reported, experimental data to verify the models are limited, due to the difficulty in measuring the dynamics at the surface itself. However, the data here show that IR is a valuable tool for monitoring the dynamics of the solute surface concentration.

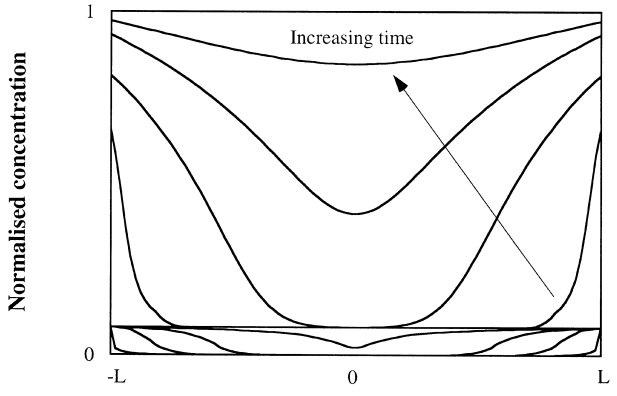

Fig. 8. Concentration profiles of propanol in BAK modelled with the equations in the theory section using the parameters given in Table 1 (highly concentration-dependent diffusivity in mode 1). The lower section refers to mode 1 and the upper section to modes 2a and 2b.

To summarize, the two-stage sorption curves presented here originate from a rapid 'sponge-like' sorption behaviour that is superimposed on a 'normal' s-shaped sorption curve. The modelled very high diffusivities of mode 1 suggest that mode 1 ends somewhere beyond the plateau of the sorption curve, which occurred only after a few minutes (see T_1 in Table 1). The modelled diffusivity of mode 1 was approximately independent of the size of the alcohol. It is therefore interesting to ask for example, why this sponge-like effect was observed here and not in *n*-hexane in polyethylene or *n*-hexane in natural rubber. One explanation might be that the polar groups of the polymer 'soak-up' the polar solutes. It is tempting to suggest that the end of mode 1 corresponded to the instant when all available polymer polar groups were 'saturated' with solute molecules, i.e. when all available carbonyl and amino groups on the polymer had formed hydrogen bonds with the hydroxyl groups on the alcohols. In parallel, solute molecules move into the 'functional-group saturated' polymer and these solutes are responsible for the mechanisms that lead to the superimposed simple s-shaped sorption curve (modes 2a and 2b). Thus, provided the first solute molecules were retarded when attached to the hydrogen bonds of the polymer, it seems reasonable to suggest that the solute molecule population consists of two groups responsible for the occurrence of respectively modes 1 and 2 (a and b). This view is similar to the dual mode sorption and mobility concepts.

5. Conclusions

It was possible to model the two-stage sorption using a time-dependent solute surface concentration, similar to that which has been used for simple s-shaped sorption curves. The time-dependence of the solute surface concentration

was verified by IR spectroscopy. This time-dependence increased exponentially with increasing size of the alcohol. The two-stage curve was considered to be due to two overlapping processes, a very rapid diffusion (mode 1) superimposed onto a normal s-shaped sorption curve (mode 2). The solubility of the alcohols in the polymer increased with increasing hydroxyl-group density, referring to the pure liquids. The alcohol diffusivity decreased non-linearly with increasing length of the molecule.

Acknowledgements

Elopak, AssiDomän, Peterson Barriere, StoraEnso, Iggesund Paperboard and the Swedish National Board for Industrial and Technical Development (VINNOVA) are thanked for the financial support.

References

[1] Hedenqvist MS, Gedde UW. Polymer 1999;40:2381.
[2] Crank J. The mathematics of diffusion. Oxford: Clarendon Press, 1986.
[3] Wind MM, Lenderink HJW. Progr Org Coat 1996;28:239.
[4] Sun Y-M. Polymer 1996;37:3921.
[5] Tang PH, Durning CJ, Guo CJ, DeKee D. Polymer 1997;38:1845.
[6] Huang SJ, Durning CJ, Freeman BD. J Polym Sci 1998;143:1.
[7] van der Vel GK, Adan OCG. Progr Org Coat 1999;37:1.
[8] Boom JP, Sanopoulou M. Polymer 2000;41:8641.
[9] Hoyt MA, Balik CM. Polym Engng Sci 1996;36:1862.
[10] Long FA, Richman D. J Am Chem Soc 1960;82:513.
[11] Berens AR, Hopfenberg HB. Polymer 1978;19:489.
[12] Kang YS, Meldon JH, Sung N. J Polym Sci: Polym Phys Ed 1990;28:1093.
[13] Bakhouya A, Brouzi AE, Bouzon J, Vergnaud JM. Plast Rubber Comp Proc Appl 1993;19:77.
[14] Edsberg L, Wedin PÅ. Optim Meth Soft 1997.
[15] Hairer E, Nørsett SP, Wanner G. Solving ordinary differential equations. Berlin: Springer, 1993.
[16] Kahaner D, Moler C, Nash S. Numerical methods and software. Englewood Cliffs: Prentice-Hall, 1989.
[17] Fleischer G. Colloid Polym Sci 1984;264:919.
[18] Gedde UW. Polymer physics. London: Chapman & Hall, 1995.
[19] Krevelen DWV. Properties of polymers. Amsterdam: Elsevier, 1990.
[20] Coates J. In: Meyers RA, editor. Encyclopedia of analytical chemistry. New York: Wiley, 2000.
[21] BAK. Technical data sheet from Bayer.
[22] Razumovskii LP, Markin VS, Zaikov GY. Polym Sci USSR 1985:27.
[23] Michaels AS, Bixler HJ. J Polym Sci 1961;5:413.